

# State estimation of wastewater treatment plants based on reduced-order model

Xunyuan Yin\*, Jinfeng Liu\*,<sup>1</sup>

\* *Department of Chemical & Materials Engineering, University of Alberta, Edmonton, AB T6G 1H9, Canada.*

---

**Abstract:** In this paper, we consider state estimation of wastewater treatment plants based on model approximation. A wastewater treatment plant described by the Benchmark Simulation Model No.1 (BSM1) is used. We use the proper orthogonal decomposition approach with re-identification of output equations to obtain a reduced-order model for the original system and then use the reduced-order model in state estimation. An approach on how to determine an appropriate minimum measurement set is also proposed. A continuous-discrete extended Kalman filtering algorithm is used to design an estimator based on the reduced-order model with re-identified output equations. The estimator gives good state estimates for the actual process.

*Keywords:* State estimation, wastewater treatment plants, model approximation, proper orthogonal decomposition, observability.

---

## 1. INTRODUCTION

Wastewater treatment plants (WWTPs) have been widely used to minimize the environmental impacts of wastewater and to recycle water (Han and Qiao (2013)). The inlet flow rate and the composition of the wastewater to a WWTP vary dramatically, which pose great challenges to the control and monitoring for WWTPs. Various model predictive control (MPC) algorithms were used for WWTPs. Set-point tracking MPC was used to control the effluent quality (Shen et al. (2008)). In Zeng and Liu (2015), an economic MPC algorithm was proposed to improve the effluent quality while minimizing the operating cost.

Most existing control approaches for WWTPs were proposed based on an assumption that all the states are measurable. This limitation can be relaxed by using state estimation. There are already some results on state estimation for WWTP related problems. In Kiss et al. (2011), a state estimator was designed for biological process models containing no more than ten state variables. Extended Kalman filter (EKF) and moving horizon estimation have been used to handle the state estimation of WWTPs based on a simplified model (Busch et al. (2013)). A distributed EKF scheme comprising two local estimators was developed based on the same simplified model (Zeng et al. (2016)). However, BSM1 which provides better description of the WWTP dynamics has not been systematically considered in state estimation. In this work, we will focus on state estimation of the BSM1 Alex et al. (2008).

The challenges are threefold: (1) state estimation problems are much more challenging when higher order models are considered (Busch et al. (2013)); (2) the future synthesis of state estimation and MPC/EMPC in one integration can be very computationally demanding based on a large-scale model (Christofides et al. (2013)); (3) by choosing

measurements following Alex et al. (2008), the BSM1 model is not locally observable. The above limitations may be bypassed if we are able to find a reduced-order model which accurately approximates the dynamics of a large-scale WWTP model and then design a state estimation scheme based on the reduced-order model (Daoutidis et al. (2016)). In addition, state estimation based on a reduced-order model may require much less measurements, which is favorable for implementation and maintenance.

In this work, we propose a systematic state estimation approach for WWTPs based on model approximation. The BSM1 model is considered. Specifically, the proper orthogonal decomposition (POD) approach is applied to obtain a reduced-order model which approximates the dynamics of the WWTP. Then, we use ordinary least squares to re-identify the output equations of the reduced-order model. The updated reduced-order model is then used in state estimation. An approach to determine a minimum set of measurements is also developed. Based on the obtained reduced-order model with selected measurements, we design a state estimation scheme using a continuous-discrete extended Kalman filtering algorithm. The simulation results show that our proposed approach can provide good state estimates of the actual dynamics of the WWTP based on only three measurements. Moreover, the computational load of the proposed scheme is substantially reduced.

## 2. PRELIMINARIES

### 2.1 Notation

$D^H$  represents the conjugate transpose of a matrix  $D$ .  $\Lambda(D)$  represents the set which contains all the eigenvalues of a matrix  $D$ .  $\lambda_i(D)$  indicates the  $i$ -th eigenvalue of a matrix  $D$ .  $\|D\|_2$  is the spectral norm of matrix  $D$ .  $\mathbb{K}_+$  represents a set that contains all non-negative integers.  $\text{diag}(v)$  is a diagonal matrix in which the elements of the

<sup>1</sup> Corresponding author: Jinfeng Liu. Tel.: +1-780-492-1317. Fax: +1-780-492-2881. Email: jinfeng@ualberta.ca.

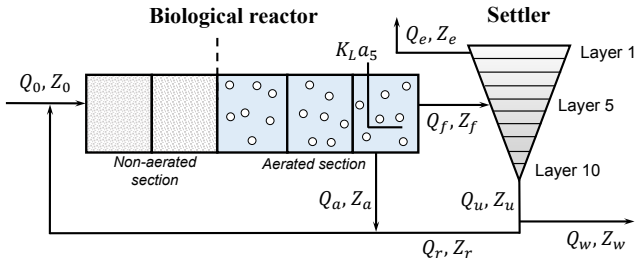


Fig. 1. A schematic of the BSM1 wastewater treatment plant

vector  $v$  are on its main diagonal. For two matrices (or vectors)  $A$  and  $B$  of the same dimension, the operator  $A \circ B$  denotes the Hadamard product which is calculated element by element as  $(A \circ B)_{i,j} = A_{i,j} \times B_{i,j}$ .  $A \circ A$  is called the Hadamard power of  $A$  and is denoted by  $A^{\circ 2}$ .

### 2.2 Wastewater treatment process description

A schematic of the WWTP based on BSM1 is presented in Fig. 1 (Alex et al. (2008)). The process comprises a multi-chamber biological activated sludge reactor and a secondary settler. The biological reactor has two sections: the non-aerated section containing the first two anoxic chambers and the aerated section consisting of the remaining three chambers. The dynamics of the settler is modeled based on mass balances of the sludge considering solid flux. A detailed description of the model of WWTPs and the process parameters can be found in (Alex et al. (2008)).

In this model, eight basic biological reaction processes are considered, and 13 major compounds are taken into account in these reactions. The concentrations of the 13 compounds in the five chambers are the state variables of the model of the biological reactor.

### 2.3 Available measurements for state estimation

For the WWTP, we consider that there are in total 49 measurements available for state estimation. In each chamber of the reactor, eight states/state-related variables are measurable (Busch et al. (2013); Alex et al. (2008)), including the oxygen concentration, the concentration of free and saline ammonia (i.e.,  $\text{NH}_3$  and  $\text{NH}_4^+$ ), nitrate and nitrate nitrogen concentration, alkalinity concentration, COD, filtered chemical oxygen demand (denoted as  $\text{COD}_f$ ), BOD. In the secondary settler, the concentrations of oxygen, free and saline ammonia, nitrate and nitrate nitrogen, and alkalinity in the top and the bottom layers, as well as the filtered chemical oxygen demand in the bottom layer are considered to be measurable.

### 2.4 Compact form of the WWTP model

The WWTP model can be described by a compact nonlinear state-space model as follows:

$$\begin{aligned} \dot{x}(t) &= f(x(t), u(t)) \\ y(t) &= Cx(t) \end{aligned} \quad (1)$$

where  $x \in \mathbb{R}^{145}$  denotes the state vector,  $y \in \mathbb{R}^{49}$  represents the vector of all the measurements,  $u \in \mathbb{R}^3$  denotes the input vector consisting of both the manipulated inputs

and the uncontrolled input to the WWTP plant. In the present work, we will derive a reduced-order model to approximate the dynamics of the model (1). Then, we will find an appropriate minimum set of measurements used for state estimation. Based on the obtained reduced-order model and the measurements from the appropriate minimum set, we design an EKF estimator to provide state estimates for the WWTP.

## 3. PROPER ORTHOGONAL DECOMPOSITION AND ITS APPLICATION TO WWTP

There are 145 state variables in the BSM1 model, and 49 measurements available for state estimation. However, by checking the rank of the observability gramian at each point along a typical state trajectory, the WWTP system is not always locally observable based on the 49 measurements. Using a reduced-order model to approximate the actual dynamics of the process and designing a state estimator based on the reduced-order model may help us bypass the observability issue.

### 3.1 Proper orthogonal decomposition

For nonlinear systems described by ordinary differential equations, a POD-based model approximation approach is introduced as follows (Antoulas and Sorensen (2001)).

Let us take into account general nonlinear systems described by Eq.(1). Based on a typical input trajectory, the corresponding state trajectory is captured and sampled every time interval  $\delta$ . Accordingly, a matrix of the sampled process states from  $t_0$  to  $t_N$  is obtained as:

$$\mathcal{X} = [x(t_0) \ x(t_1) \ \dots \ x(t_N)] \quad (2)$$

where  $\mathcal{X} \in \mathbb{R}^{n \times (N+1)}$  is called a snapshot matrix of the actual state. In (2),  $n$  represents the number of state variables, while  $N$  is the number of sampling intervals. For the snapshot matrix  $\mathcal{X}$ , we require that the number of samples should be sufficiently large such that  $N \gg n$ . At the next step, singular value decomposition (SVD) is performed on the matrix  $\mathcal{X}$  as:

$$\mathcal{X} = U \Sigma V^H \quad (3)$$

where  $U$  is a  $n \times n$  unitary matrix,  $\Sigma$  is an  $n \times (N+1)$  rectangular matrix with non-negative real values on its main diagonal,  $V$  is an  $(N+1) \times (N+1)$  unitary matrix. The entries  $\sigma_i$ ,  $i \in \{1, \dots, n\}$ , on the main diagonal of  $\Sigma$  are the singular values of matrix  $\mathcal{X}$ . Commonly,  $\sigma_i$ ,  $i \in \{1, \dots, n\}$ , are arranged in a descending order on the main diagonal of  $\Sigma$ . Subsequently, we should check if these values decrease rapidly. If yes, then do the following steps:

- (1) Select an appropriate positive integer  $r < 145$ , such that the first  $r$  singular values  $\sigma_i$ ,  $i \in \{1, \dots, r\}$  are much larger than the remained singular values;
- (2) Obtain a reduced-order square matrix  $\Sigma_r$  by truncating the matrix  $\Sigma$  at the  $r$ -th column and row;
- (3) Select the first  $r$  columns of  $U$  to form a matrix  $U_r$ ;
- (4) Select the first  $r$  rows of  $V^H$  to form a matrix  $V_r^H$ .

Then, a lower-order approximation of the actual process data is formed as

$$\mathcal{X} \approx U_r \Sigma_r V_r^H \quad (4)$$

Let us use  $\xi \in \mathbb{R}^r$  to denote the state vector of the reduced-order model, and define  $\xi(t) := U_r^H x(t)$ . By considering the

original nonlinear model in Eq.(1), a reduced-order model of order  $r$  is expressed in the following state-space form:

$$\dot{\xi}(t) = f_r(\xi(t), u(t)) \quad (5a)$$

$$y(t) = CU_r\xi(t) \quad (5b)$$

where  $f_r$  denotes a vector field which is defined as  $f_r(\xi, u) := U_r^H f(U_r\xi, u)$ . Based on the evolution of  $\xi(t)$  in model (5), the actual state trajectory of the original nonlinear process can be approximated through the mapping  $x(t) \approx U_r\xi(t)$ .

### 3.2 Model reduction of the WWTP

For WWTP,  $Q_0$  (and  $Z_0$ ) is an input that is primarily determined by the current weather condition;  $Q_a$  and  $K_{La5}$  are two manipulated inputs that are usually used in control system designs. When the weather conditions are different, the values of  $Q_0$  and  $Z_0$  are much different. Note that a different model should be identified for each weather condition accordingly to accurately approximate the dynamics under different weather conditions.

To perform model order reduction, the three inputs are used to excite the WWTPs. The input sequence of  $Q_0$  and the associated concentration information  $Z_0$  are obtained from real data under the dry-weather condition. We consider that the input  $Q_a$  is a periodic (with a period of 1 day) RBS taking a value of either  $5.5338 \times 10^4 \text{ m}^3 \cdot \text{d}^{-1}$  or  $1.6601 \times 10^5 \text{ m}^3 \cdot \text{d}^{-1}$ ; the input  $K_{La5}$  is also a RBS which takes a value of either  $84 \text{ d}^{-1}$  or  $252 \text{ d}^{-1}$ . The initial condition of the process is selected as the steady-state which is corresponding to constant inputs  $[Q_0 \ Q_a \ K_{La5}]^T = [18446 \ 55338 \ 84]^T$ . The input signals are applied to the WWTP process to generate the state trajectories which are sampled every 1 min (i.e.,  $\delta = 1 \text{ min}$ ). The sampled states within the first 28 days are used to construct the snapshot matrix  $\mathcal{X}$  for POD analysis. In this case, the number of sampling intervals is 40320 and the requirement  $N \gg n$  is satisfied.

Then, SVD is performed on the matrix  $\mathcal{X}$  of a dimension 145 by 40321 and a unitary matrix  $U$  used for coordinate transformation is obtained. The next step is to select a proper order for the reduced model. When determining the order of the reduced-order model, we strike a balance between the size of the model and the accuracy of the model, the latter of which cannot be directly checked by examining the singular values.

To evaluate the reduced-order model accuracy, we resort to the criterion based on the  $H_2$  norm of the model errors. The  $H_2$  index (denoted by  $|e_{\text{model}}|_{H_2}$ ) which serves as an indicator of the model mismatch is defined as follows:

$$|e_{\text{model}}|_{H_2} := \sqrt{\sum_{k=0}^N \sum_{i=1}^{145} \left( \frac{x_i(t_k) - \bar{x}_i(t_k)}{x_i(t_k)} \right)^2} \quad (6)$$

where  $x_i$  represents the  $i$ -th state involved in the state vector  $x$ ,  $\bar{x} := U_r\xi$  is the approximated state obtained from a reduced order model, and  $\bar{x}_i$  is the  $i$ -th element in  $\bar{x}$  which is associated with  $x_i$ ,  $i \in \{1, \dots, 145\}$ .

To determine the accuracy of a reduced-order model, we simulate the actual process over a period of 14 days with  $Q_a$  and  $K_{La5}$  determined by two PI controllers as specified

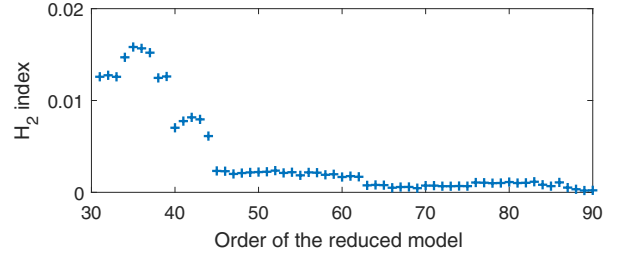


Fig. 2. The values of the  $H_2$  index at different orders

in Zeng and Liu (2015). The trajectories of  $Q_a$  and  $K_{La5}$  are recorded. The same  $Q_a$ ,  $K_{La5}$  trajectories as well as the same weather condition  $Q_0$  are applied to each reduced-order model in an off-line manner to obtain the corresponding state trajectories.

Based on the actual process state trajectories and reduced-order model state trajectories, the  $H_2$  index is calculated for each model. The values of the  $H_2$  index at different orders  $r = 30, \dots, 90$  are shown in Fig. 2. In general, the degree of model mismatch increases with the decrease in the model order. Moreover, the  $H_2$  index remains at a comparatively low level when the order is no less than 40. By further examining the values of this index with respect to different orders, we determine to use the reduced model with order 45 for state estimation. That is, the leading 45 columns of the matrix  $U$  are used to constitute the coordinate transformation matrix  $U_r$  in reduced model (5).

## 4. OUTPUT EQUATION RE-IDENTIFICATION AND MEASUREMENT SELECTION

In this section, we propose to re-identify the output equation of the reduced-order model for improved model accuracy and propose an approach to determine the measurement set used in estimation.

### 4.1 Re-identification of the output equation

The use of a reduced-order model to approximate the actual process dynamics leads to model mismatch. To improve the accuracy of the reduced-order model, we re-identify the output model. This is based on the fact that the output model was derived from (5a) and the actual system measurements were not used, which makes (5b) not a very good approximation of the relation between the actual measurement and the reduced-order model states. To improve the accuracy of the output model, we can re-identify the output equation using the actual output measurements and the reduced-order model states.

We examine the trajectories of the actual measurements and the approximations of the measurements based on POD. While most approximations are close to the true values of the measurements, the approximations for a few measurements of  $\text{COD}_f$  at different locations (denoted by  $y_{31}$  to  $y_{36}$ ) do not track the trends of the corresponding true values very well. In Fig. 3, we present the trajectories of the true measurements with respect to  $\text{COD}_f$  (blue dash-dot lines) and their approximations given by the reduced-order model (orange dashed lines). The discrepancy is not negligible.

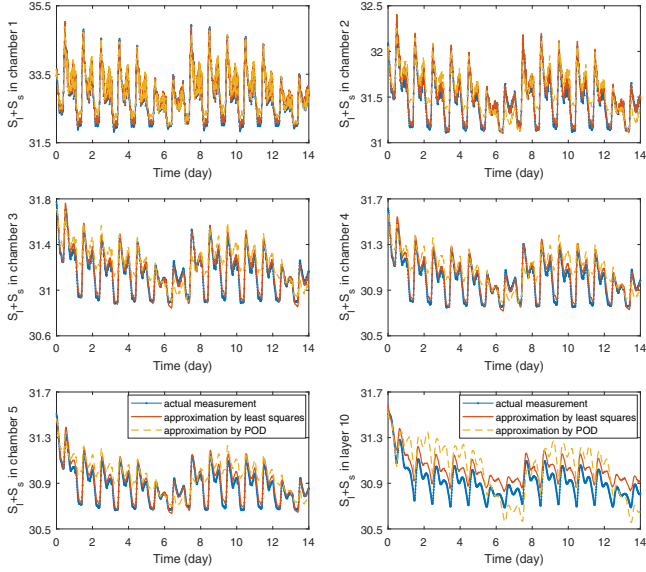


Fig. 3. The trajectories of the true measurements with respect to  $COD_f$ , the approximations based on POD and the approximations based on least squares

One way to reduce the mismatch of the model (5b) is to re-identify the output functions for the six measurements using least squares. Let us denote by  $Y(t_k)$  the vector of the six considered measurements at  $t_k$  (i.e.,  $Y(t_k) = [y_{31}(t_k) \dots y_{36}(t_k)]^T$ ) and denote by  $\xi(t_k)$  the vector of the reduced system states (i.e.,  $\xi(t_k) := [\xi_1(t_k) \dots \xi_{45}(t_k)]^T$  for  $k = 0, \dots, N$ ). Further, let  $\mathcal{Y} = [Y(t_0) \dots Y(t_N)]$  and  $\Xi = [\xi(t_0) \dots \xi(t_N)]$ . A linear model is established as:

$$\mathcal{Y}^T = \Xi^T \beta + \varepsilon \quad (7)$$

where  $\beta$  is a 45 by 6 matrix consisting of unknown parameters to be identified,  $\varepsilon$  contains unobserved random variables accounting for the discrepancy between the true observations and the corresponding approximations provided by the linear functions. Based on least squares, an estimate of the unknown parameter matrix  $\beta$  is given by the Moore-Penrose pseudo-inverse of matrix  $\Xi^T$  as:

$$\hat{\beta} = (\Xi \Xi^T)^{-1} \Xi \mathcal{Y}^T \quad (8)$$

The simulation is implemented under the same condition considered in model reduction. Specifically, using the same input signals to stimulate the reduced-order model, the corresponding state trajectory  $\Xi$  is generated. The trajectories of the six measurements under this condition are also used. Using the data  $\mathcal{Y}$  and  $\Xi$  sampled from the above trajectories, an estimate  $\hat{\beta}$  is obtained based on (8). Then, the identified output functions are validated. Let us take the dry weather condition for example. As seen from Fig. 3, the output functions for the six considered measurements updated based on least squares (red solid lines) are more accurate compared to the output functions generated from POD (orange dashed lines).

Therefore, the matrix  $\beta^T$  is used to replace the 31-rd row to the 36-th row of the matrix  $CU_r$  in Eq.(5b) such that an updated reduced-order model is generated:

$$\dot{\xi}(t) = f_r(\xi(t), u(t)) \quad (9a)$$

$$y(t) = C_r \xi(t) \quad (9b)$$

## 4.2 Measurement selection

There are in total 49 measurements that can be used for state estimation. However, the use of more measurements will lead to higher economic investment and more maintenance efforts. In this section, we discuss how to find a minimum configuration of measurements which ensures the local observability of the process. Then, we propose to select an appropriate configuration of measurements which provides improved degree of observability.

*Assessment criteria for quality of observability* We first introduce the following criteria that have been proposed for assessing the quality of observability of linear systems. These criteria provide scalar measures by using the observability gramian  $W_o$ .

Consider an imbedding set of scalar functions depending on a (semi-)positive definite matrix  $D$  described in the following form (Müller and Weber (1972)):

$$m_s = m_s(\Lambda(D)) = \left( \sum_{i=1}^n \frac{1}{n} \lambda_{i,D}^s \right)^{\frac{1}{s}} \quad (10)$$

with a proper order  $s \leq 0$  which is to be specified and  $n$  being the dimension of the matrix  $D$ . In Eq.(10),  $\lambda_{i,D}$ ,  $i \in \{1, \dots, n\}$ , represents the  $i$ -th eigenvalue of matrix  $D$ . The form in (10) that is evaluated based on the observability gramian  $W_o$  at different orders of interest leads to three evaluation criteria for the quality of observability (Müller and Weber (1972)):  $\mu_1 = \lim_{s \rightarrow -\infty} m_s(\Lambda(W_o)) = \min \{ \lambda_i(W_o) | i = 1, \dots, n_{\bar{x}} \}$ ,  $\mu_2 = m_s(\Lambda(W_o))|_{s=-1} = \frac{n_{\bar{x}}}{\text{trace}(W_o^{-1})}$  and  $\mu_3 = \lim_{s \rightarrow 0} m_s(\Lambda(W_o)) = \sqrt[n_{\bar{x}}]{\det(W_o)}$ .

Basically, for each scalar function  $\mu_i$ ,  $i = 1, 2, 3$ , a larger value for the investigated system indicates a better quality of observability of the system with the corresponding configuration of measurements.

In addition, two more criteria effective for determining the quality of observability are introduced. One is the condition number of the observability gramian (Dochain et al. (1997)). In particular, based on the observability gramian  $W_o$ , the index is calculated as:  $\gamma(W_o) = \frac{\max \{ \sigma_i : i = 1 \dots, n_{\bar{x}} \}}{\min \{ \sigma_i : i = 1 \dots, n_{\bar{x}} \}}$  where  $\sigma_i$ ,  $i \in \{1, \dots, n_{\bar{x}}\}$ , is the  $i$ -th singular value of the matrix  $W_o$ . Unlike the other criteria, a larger condition number implies that the system has weaker observability, which brings difficulty in designing a successful state estimation scheme.

The last adopted measure is the spectral norm of observability gramian  $W_o$  (Van den Berg et al. (2000)):  $\rho(W_o) = \|W_o\|_2 = \sqrt{\max \{ \sigma_i : i = 1 \dots, n_{\bar{x}} \}}$ . A larger  $\rho(W_o)$  is associated with a better observability result.

Note that when the above measures are used to compare the quality of observability of a system with different measurement configurations, this is no guarantee that the five quality indices (i.e.,  $\mu_1$ ,  $\mu_2$ ,  $\mu_3$ ,  $\gamma$  and  $\rho$ ) will give strictly consistent result. Based on this consideration, an index (denoted by OQOI) that combines the five indices via weighting coefficients is proposed to assess the overall quality of observability of a system.

$$\text{OQOI} = \frac{\mu_1}{c_1} + \frac{\mu_2}{c_2} + \frac{\mu_3}{c_3} + \frac{1}{\gamma(W_o)} + \frac{\rho(W_o)}{c_5} \quad (11)$$

where  $c_i, i = 1, \dots, 5$ , are pre-determined constant weighting coefficients. When the five individual indices cannot provide a consistent recommendation, we calculate the indices of OQOI and select the best configuration with the largest OQOI value among candidates.

#### Selection of a minimum measurement configuration

First, we linearize the reduced-order model (9) successively at different points along its operating trajectories and find the minimum number of measurements that give local observability of the reduced-order model. Then, the measure OQOI is used to determine the set of minimum measurements that gives the highest degree of observability. The detailed procedure is summarized as follow.

*Algorithm 1.* Determine the minimum measurement set

1. Generate a trajectory of the state  $\xi$  from  $t_0$  to  $t_N$  based on the reduced model (9).
2. Sample the state trajectory every sampling period  $\Delta$ .
3. At each sampling time  $t_k$ , linearize the reduced system model (9a) at the point  $(\xi(t_k), u(t_k))$  and obtain the system matrices (denoted by  $A_{\xi,k} := \left. \frac{\partial f_r(\xi, u)}{\partial \xi} \right|_{(\xi(t_k), u(t_k))}$ ,  $k = 0, \dots, N$ ).
4. Set  $m = 1$ , and perform the following steps:
  - 4.1. Find all the possible measurement configurations in each of which there is(are)  $m$  measurement(s), and form the corresponding output matrices.
  - 4.2. At  $t_k, k = 0, \dots, N$ , calculate the observability gramian  $W_o(t_k)$  for the linearized system under each possible measurement configuration.
  - 4.3. For each configuration, calculate the ranks of the associated observability gramian matrices along the trajectory and do:
    - if** the gramian matrices at  $t_k, \forall k = 0, \dots, N$ , are full-rank for only one configuration of measurement(s), **then**
      - choose this configuration as the minimum configuration for state estimation, **end**.
      - else if** the gramian matrices at  $t_k, \forall k = 0, \dots, N$ , are full-rank with respect to at least one configuration of measurement(s), **then**
        - go to Step 5.
        - else**
          - set  $m=m+1$  and go to Step 4.1.
          - end**
5. Select each measurement configuration which leads to full-rank  $W_o(t_k), \forall k = 0, \dots, N$ , calculate the mean value of OQOI along the trajectory.
6. Among the measurement configurations found in Step 5, choose a minimum configuration for state estimation with the largest average OQOI.

The weighting coefficients  $c_i, i = 1, \dots, 5$ , in OQOI in (11) are determined on a case-by-case basis. In this work, each  $c_i, i = 1, \dots, 5$ , is selected to be the largest value that the corresponding quality index can reach at  $m = 3$ . The results suggest that the minimum number of process measurements required to ensure local observability at all the sampling instants is 3. More than one configuration of

measurements is found. To select the best configuration, the indices of  $\mu_1, \mu_2, \mu_3, \gamma$  and  $\rho$  are further calculated based on the observability gramian for all the possible configurations within a 14-day period. OQOI are calculated for all the 18424 possible measurement configurations within a 14-day period. The 15200-th configuration with measurements  $y_{22}, y_{25}$  and  $y_{26}$  is recommended. In this set of simulations, for each candidate configuration, we calculate the observability gramian and calculate the corresponding indices of the quality of observability every 2 hours (i.e.,  $\Delta = 2\text{h}$ ) due to high computational burden.

## 5. STATE ESTIMATION BASED ON REDUCED-ORDER MODEL

In this section, we design a centralized EKF estimator based on the reduced-order model.

Let us consider a stochastic version of the reduced system model in (5) described as in the following form:

$$\dot{\xi}(t) = f_r(\xi(t), u(t)) + w(t) \quad (12a)$$

$$y(t) = C_r \xi(t) + v(t) \quad (12b)$$

where  $w \in \mathbb{R}^{n_\xi}$  denotes the vector of process disturbances and  $v \in \mathbb{R}^{n_y}$  represents the vector of measurement noise. We further assume that the process disturbances  $w$  and measurement noise  $v$  are two mutually uncorrelated Gaussian noise sequences and are with zero-mean and covariance matrices  $Q_w$  and  $R_v$ , respectively.

The reduced-order model is featured by continuous-time dynamics, yet only sampled measurements. Based on the above consideration, a continuous-discrete EKF estimator is designed following Frogerais et al. (2012). Within a sampling period  $t \in (t_{k-1}, t_k]$ , in the predictor-update step, a prediction (i.e.,  $\hat{\xi}(t|t_{k-1})$ ) is given in an open-loop manner based on the reduced-order model (5a) and initial condition  $\hat{\xi}(t_{k-1}|t_{k-1})$ . Then, at each sampling instant  $t_k$ , a state estimate of the actual dynamics of the reduced system (denoted as  $\hat{\xi}(t_k, t_k)$ ) is obtained by performing the measurement-update step. By taking advantage of the discrete state estimate given by EKF (denoted as  $\hat{\xi}$ ) and the linear mapping  $U_r$ , the state estimate of the actual state of the WWTPs (denoted by  $\hat{x}$ ) is obtained following  $\hat{x}(t_k) = U_r \hat{\xi}(t_k), k \in \mathbb{K}_+$ .

## 6. SIMULATIONS

### 6.1 Simulation settings

The data for different weather conditions were obtained from the International Water Association website. The values of the process parameters are selected to be the same as given in Alex et al. (2008).

The measurements are sampled synchronously at  $t_{n \geq 0}$  where  $t_n = t_0 + n\Delta_s$  with  $t_0 = 0$  the initial time instant,  $\Delta_s = 15\text{min}$  the sampling period and  $n \in \mathbb{K}_+$ . At each sampling instant, the measurements are immediately available to the estimator. Each process disturbance sequence associated with the  $i$ -th state  $x_i$  is generated following normal distribution with zero mean and standard deviation  $0.1x_{i,s}$  where  $x_{i,s}$  is the steady-state value of  $x_i$  corresponding to specific constant inputs. Random noise to each

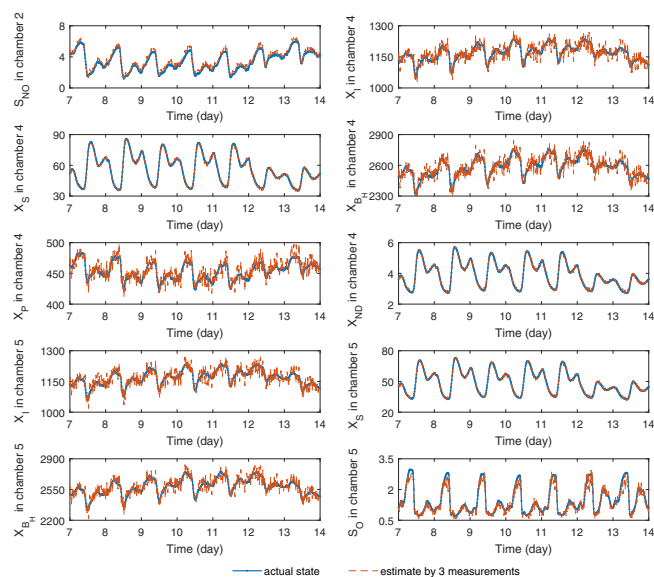


Fig. 4. The trajectories of the actual states (blue dash dot lines) and the state estimates based on 3 measurements (red dashed lines) in dry weather

measurement  $y_i$  is Gaussian white noise with zero mean and standard deviation  $0.08y_{i,s}$ , in which  $y_{i,s}$  is the value of  $y_i$  at steady-state. The tuning parameters in the EKF are  $Q_w = \text{diag}(v_w^2)$  where  $v_w = 0.1 \times U_r^H [x_{1,s} \dots x_{145,s}]$  and  $R_v = \text{diag}(v_v^2)$  where  $v_v = 0.08 \times U_r^H [y_{1,s} \dots y_{49,s}]$ .

### 6.2 Results of dry weather condition

We consider state estimation with the minimum measurement set in dry weather for illustration. Some of the trajectories of the state estimates and the actual states are shown in Fig. 4. The proposed estimation scheme with three measurements can give good estimates.

We also compare the proposed scheme with a centralized EKF scheme directly designed based on the BSM1 model in terms of computational efficiency. The average computation time required by the proposed EKF scheme with 3 measurements and the EKF explicitly based on the BSM1 model is 780.46 sec and 3345.62 sec, respectively. The proposed approach is more computationally efficient due to the use of the reduced-order model.

## 7. CONCLUDING REMARKS

State estimation for WWTP was addressed via POD-based model approximation. The output functions in the reduced model were updated using least squares for improved accuracy. We also proposed an algorithm to determine a minimum set of measurements for state estimation. An EKF-based state estimation scheme was developed using the reduced model and the formed measurement set. Simulations were carried out under the dry weather condition. The good estimates of the actual WWTP dynamics demonstrated the effectiveness the proposed approach.

## ACKNOWLEDGMENT

Financial support from Natural Sciences and Engineering Research Council of Canada and Alberta Innovates Technology Futures is gratefully acknowledged.

## REFERENCES

- Alex, J., Benedetti, L., Copp, J., Gernaey, K.V., Jeppsson, U., Nopens, I., Pons, M.N., Rieger, L., Rosen, C., Steyer, J.P., Vanrolleghem, P., and Winkler, S. (2008). Benchmark simulation model no. 1 (BSM1). *Technical Report, Department of Industrial Electrical Engineering and Automation, Lund University*.
- Antoulas, A.C. and Sorensen, D.C. (2001). Approximation of large-scale dynamical systems: An overview. *International Journal of Applied Mathematics and Computer Science*, 11, 1093–1121.
- Busch, J., Elixmann, D., Kühl, P., Gerken, C., Schlöder, J.P., Bock, H.G., and Marquardt, W. (2013). State estimation for large-scale wastewater treatment plants. *Water Research*, 47(13), 4774–4787.
- Christofides, P.D., Scattolini, R., Muñoz de la Peña, D., and Liu, J. (2013). Distributed model predictive control: A tutorial review and future research directions. *Computers & Chemical Engineering*, 51, 21–41.
- Daoutidis, P., Zachar, M., and Jogwar, S.S. (2016). Sustainability and process control: A survey and perspective. *Journal of Process Control*, 44, 184–206.
- Dochain, D., Tali-Maamar, N., and Babary, J.P. (1997). On modelling, monitoring and control of fixed bed bioreactors. *Computers & Chemical Engineering*, 21(11), 1255–1266.
- Frogerais, P., Bellanger, J.J., and Senhadji, L. (2012). Various ways to compute the continuous-discrete extended Kalman filter. *IEEE Transactions on Automatic Control*, 57(4), 1000–1004.
- Han, H. and Qiao, J. (2013). Hierarchical neural network modeling approach to predict sludge volume index of wastewater treatment process. *IEEE Transactions on Control Systems Technology*, 21(6), 2423–2431.
- Kiss, A.M.N., Marx, B., Mourot, G., Schutz, G., and Ragot, J. (2011). State estimation of two-time scale multiple models. application to wastewater treatment plant. *Control Engineering Practice*, 19(11), 1354–1362.
- Müller, P.C. and Weber, H.I. (1972). Analysis and optimization of certain qualities of controllability and observability for linear dynamical systems. *Automatica*, 8(3), 237–246.
- Shen, W., Chen, X., and Corriou, J.P. (2008). Application of model predictive control to the BSM1 benchmark of wastewater treatment process. *Computers & Chemical Engineering*, 32(12), 2849–2856.
- Van den Berg, F.W.J., Hoefsloot, H.C.J., Boelens, H.F.M., and Smilde, A.K. (2000). Selection of optimal sensor position in a tubular reactor using robust degree of observability criteria. *Chemical Engineering Science*, 55(4), 827–837.
- Zeng, J. and Liu, J. (2015). Economic model predictive control of wastewater treatment processes. *Industrial & Engineering Chemistry Research*, 54(21), 5710–5721.
- Zeng, J., Liu, J., Zou, T., and Yuan, D. (2016). Distributed extended Kalman filtering for wastewater treatment processes. *Industrial & Engineering Chemistry Research*, 55(28), 7720–7729.